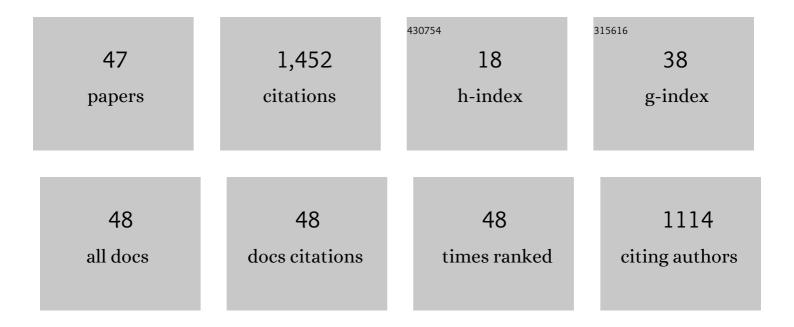
Yutaro Takaya

List of Publications by Year in descending order

Source: https://exaly.com/author-pdf/9118683/publications.pdf Version: 2024-02-01



#	Article	IF	CITATIONS
1	Deep-sea mud in the Pacific Ocean as a potential resource for rare-earth elements. Nature Geoscience, 2011, 4, 535-539.	5.4	434
2	The tremendous potential of deep-sea mud as a source of rare-earth elements. Scientific Reports, 2018, 8, 5763.	1.6	157
3	Uranium isotope systematics of ferromanganese crusts in the Pacific Ocean: Implications for the marine 238U/235U isotope system. Geochimica Et Cosmochimica Acta, 2014, 146, 43-58.	1.6	85
4	Discovery of extremely REY-rich mud in the western North Pacific Ocean. Geochemical Journal, 2016, 50, 557-573.	0.5	68
5	Postâ€drilling changes in fluid discharge pattern, mineral deposition, and fluid chemistry in the Iheya North hydrothermal field, Okinawa Trough. Geochemistry, Geophysics, Geosystems, 2013, 14, 4774-4790.	1.0	52
6	Rare-earth, major, and trace element geochemistry of deep-sea sediments in the Indian Ocean: Implications for the potential distribution of REY-rich mud in the Indian Ocean. Geochemical Journal, 2015, 49, 621-635.	0.5	51
7	Geological factors responsible for REY-rich mud in the western North Pacific Ocean: Implications from mineralogy and grain size distributions. Geochemical Journal, 2016, 50, 591-603.	0.5	46
8	Rapid growth of mineral deposits at artificial seafloor hydrothermal vents. Scientific Reports, 2016, 6, 22163.	1.6	44
9	Geochemistry of REY-rich mud in the Japanese Exclusive Economic Zone around Minamitorishima Island. Geochemical Journal, 2016, 50, 575-590.	0.5	42
10	Post-Drilling Changes in Seabed Landscape and Megabenthos in a Deep-Sea Hydrothermal System, the Iheya North Field, Okinawa Trough. PLoS ONE, 2015, 10, e0123095.	1.1	41
11	A new and prospective resource for scandium: Evidence from the geochemistry of deep-sea sediment in the western North Pacific Ocean. Ore Geology Reviews, 2018, 102, 260-267.	1.1	41
12	Marine osmium isotope record during the Carnian "pluvial episode―(Late Triassic) in the pelagic Panthalassa Ocean. Global and Planetary Change, 2021, 197, 103387.	1.6	33
13	Fish proliferation and rare-earth deposition by topographically induced upwelling at the late Eocene cooling event. Scientific Reports, 2020, 10, 9896.	1.6	29
14	Quantitative in situ mapping of elements in deep-sea hydrothermal vents using laser-induced breakdown spectroscopy and multivariate analysis. Deep-Sea Research Part I: Oceanographic Research Papers, 2020, 158, 103232.	0.6	28
15	Signal preprocessing of deep-sea laser-induced plasma spectra for identification of pelletized hydrothermal deposits using Artificial Neural Networks. Spectrochimica Acta, Part B: Atomic Spectroscopy, 2018, 145, 1-7.	1.5	26
16	Major and trace element compositions and resource potential of ferromanganese crust at Takuyo Daigo Seamount, northwestern Pacific Ocean. Geochemical Journal, 2016, 50, 527-537.	0.5	26
17	Re–Os isotope geochemistry in the surface layers of ferromanganese crusts from the Takuyo Daigo Seamount, northwestern Pacific Ocean. Geochemical Journal, 2015, 49, 233-241.	0.5	23
18	Removal mechanisms of arsenite by coprecipitation with ferrihydrite. Journal of Environmental Chemical Engineering, 2021, 9, 105819.	3.3	21

ΥUTARO ΤΑΚΑΥΑ

#	Article	IF	CITATIONS
19	REY-Rich Mud. Fundamental Theories of Physics, 2015, , 79-127.	0.1	17
20	Subseafloor sulphide deposit formed by pumice replacement mineralisation. Scientific Reports, 2021, 11, 8809.	1.6	17
21	A Miocene impact ejecta layer in the pelagic Pacific Ocean. Scientific Reports, 2019, 9, 16111.	1.6	15
22	Chemical leaching of rare earth elements from highly REY-rich mud. Geochemical Journal, 2015, 49, 637-652.	0.5	15
23	A Study on the Recovery Method of Rare-Earth Elements from REY-Rich Mud toward the Development and the Utilization of REY-Rich Mud. Journal of MMIJ, 2014, 130, 104-114.	0.4	15
24	Zircon U–Pb dating from the mafic enclaves in the Tanzawa Tonalitic Pluton, Japan: Implications for arc history and formation age of the lower-crust. Lithos, 2014, 196-197, 301-320.	0.6	14
25	Origin of felsic volcanism in the Izu arc intra-arc rift. Contributions To Mineralogy and Petrology, 2017, 172, 1.	1.2	13
26	A Combination of Geostatistical Methods and Principal Components Analysis for Detection of Mineralized Zones in Seafloor Hydrothermal Systems. Natural Resources Research, 2021, 30, 2875-2887.	2.2	11
27	Dissolution of altered tuffaceous rocks under conditions relevant for CO2 storage. Applied Geochemistry, 2015, 58, 78-87.	1.4	8
28	Biotic and environmental changes in the Panthalassa Ocean across the Norian (Late Triassic) impact event. Progress in Earth and Planetary Science, 2020, 7, .	1.1	8
29	Geological, geochemical and social-scientific assessment of basaltic aquifers as potential storage sites for CO2. Geochemical Journal, 2013, 47, 385-396.	0.5	7
30	Triassic marine Os isotope record from a pelagic chert succession, Sakahogi section, Mino Belt, southwest Japan. Journal of Asian Earth Sciences: X, 2019, 1, 100004.	0.6	7
31	Depositional Age of a Fossil Whale Bone from São Paulo Ridge, South Atlantic Ocean, Based on Os Isotope Stratigraphy of a Ferromanganese Crust. Resource Geology, 2017, 67, 442-450.	0.3	6
32	Formation of highly Zn-enriched sulfide scale at a deep-sea artificial hydrothermal vent, Iheya-North Knoll, Okinawa Trough. Mineralium Deposita, 2021, 56, 975.	1.7	6
33	Purification of calcium fluoride (CaF2) sludge by selective carbonation of gypsum. Journal of Environmental Chemical Engineering, 2021, 9, 104510.	3.3	6
34	Progressive ocean oxygenation atÂ~2.2ÂGa inferred from geochemistry and molybdenum isotopes of the Nsuta Mn deposit, Ghana. Chemical Geology, 2021, 567, 120116.	1.4	6
35	3D geostatistical modeling of metal contents and lithofacies for mineralization mechanism determination of a seafloor hydrothermal deposit in the middle Okinawa Trough, Izena Hole. Ore Geology Reviews, 2021, 135, 104194.	1.1	6
36	Longâ€Term Reaction Characteristics of CO ₂ –Water–Rock Interaction: Insight into the Potential Groundwater Contamination Risk from Underground CO ₂ Storage. Resource Geology, 2018, 68, 93-100.	0.3	5

ΥUTARO ΤΑΚΑΥΑ

#	Article	IF	CITATIONS
37	Umber as a lithified REY-rich mud in Japanese accretionary complexes and its implications for the osmium isotopic composition of Middle Cretaceous seawater. Ore Geology Reviews, 2022, 142, 104683.	1.1	5
38	Mechanochemical degradation treatment of TBBPA: A kinetic approach for predicting the degradation rate constant. Advanced Powder Technology, 2022, 33, 103469.	2.0	4
39	Unique Environmental Conditions Required for Dawsonite Formation: Implications from Dawsonite Synthesis Experiments under Alkaline Conditions. ACS Earth and Space Chemistry, 2019, 3, 285-294.	1.2	3
40	Experiments on Rare-Earth Element Extractions from Umber Ores for Optimizing the Grinding Process. Minerals (Basel, Switzerland), 2019, 9, 239.	0.8	3
41	Prediction of Acid Mine Drainage Treatment by Open Limestone-Alkaline Material Channel and Implications for the Large Scale Implementation of Passive Treatment. Journal of MMIJ, 2022, 138, 19-27.	0.4	3
42	Re–Os geochemistry of hydrothermally altered dacitic rock in a submarine volcano at Site U1527, IODP Expedition 376: Implications for the Re cycle in intraoceanic arcs. Deep-Sea Research Part I: Oceanographic Research Papers, 2022, 180, 103687.	0.6	2
43	Geochemical Trapping of CO2 in Basaltic Aquifers: Implications from CO2-Water-Rock Interaction Experiments. Journal of MMIJ, 2010, 126, 131-137.	0.4	1
44	Kinetic Evaluation of pH and Temperature Effects on Silica Polymerization in the Presence of Mg, Al and Fe. Kagaku Kogaku Ronbunshu, 2021, 47, 237-244.	0.1	1
45	Impact of Biodegradable Plastics, Especially PHBH, on Mechanical Recycling. Resources Processing, 2022, 68, 143-149.	0.4	1
46	Simplified Prediction of the Proceeding of Mineral Trapping of CO2 Based on Experimental Study. Journal of MMIJ, 2012, 128, 94-102.	0.4	0
47	Derivation of Flotation Kinetic Model Combining Surface Property Analysis and Kinetics. Journal of MMIJ, 2022, 138, 12-18.	0.4	0